

INVERSE MEASUREMENT OF THERMAL BOUNDARY CONDITIONS USING A TRANSIENT TEMPERATURE HISTORY

K. MOMOSE, K. ABE and H. KIMOTO

Department of Mechanical Science and Bioengineering, Graduate School of Engineering Science

Osaka University, Osaka 560-8531, Japan

e-mail: momose@me.es.osaka-u.ac.jp

Abstract - A non-iterative approach based on adjoint formulation of conduction heat transfer is proposed to identify the thermal boundary conditions from a transient temperature history measured in a solid body. Using a numerical solution of the adjoint problem, which can be regarded as a numerical Green's function, the temperature at the measuring point can be evaluated under arbitrary thermal boundary conditions. As a result, we can inversely predict the thermal boundary conditions from the measured temperature history by assuming the step-wise profiles of thermal boundary conditions and by using a regularization method to stabilize the resulting discrete ill-posed problem.

1. INTRODUCTION

Since inverse heat conduction problems (IHCP) arise in many areas of engineering and science, a number of solution methods have been developed for the IHCP[1, 2]; especially, the inverse problem of estimating the thermal boundary conditions from temperature measurements in a heat conducting body is constantly of a great interest[4]. For this kind of problem, optimization strategies are often applied, in which the differences between the measured temperatures and simulated ones are iteratively minimized. In such methods, however, a large number of numerical simulations for the heat conduction field are required in the iterative optimization process.

In this study, a non-iterative approach based on adjoint formulation of conduction heat transfer is proposed, the goal of which is to identify the thermal boundary conditions from a single transient temperature history measured in a heat conducting body. The first step for developing the present method is to formulate the general relationship between the thermal boundary conditions and the temperature at the measuring point. We use the weak formulation of heat conduction problem to derive the relationship. Then, by using a numerical solution of the associated adjoint problem, which can be regarded as a numerical Green's function, the temperature at the measuring point can be evaluated under arbitrary thermal boundary conditions. In the inverse step, assuming the step-wise profiles of the thermal boundary conditions, we can non-iteratively determine the thermal boundary conditions in the least squares sense. Moreover, to stabilize the ill-posed problem appeared in the present approach, we will discuss Tikhonov regularization method. The results of computational experiments in a two-dimensional heat conduction problem are presented to demonstrate the present method.

2. PROBLEM FORMULATION

Consider a finite solid body with constant material properties, and let Ω be an inner domain and Γ its boundary. Then the heat conduction equation can be written in a dimensionless form as

$$\frac{\partial T(\mathbf{x}, t)}{\partial t} = \nabla^2 T(\mathbf{x}, t) \quad (1)$$

where T is the temperature, \mathbf{x} is the space vector, and t is the time.

Here, we introduce a temperature $\theta(\mathbf{x}, t)$ defined as the difference from a known harmonic initial temperature distribution, and we suppose that the boundary Γ consists of the temperature-specified boundary Γ_θ and the heat-flux-specified boundary Γ_q . Then, the governing equation and the initial and boundary conditions adopted in this study can be summarized as follows:

$$\frac{\partial \theta(\mathbf{x}, t)}{\partial t} = \nabla^2 \theta(\mathbf{x}, t) \quad \mathbf{x} \in \Omega, t > 0 \quad (2)$$

$$\theta(\mathbf{x}, 0) = 0 \quad \mathbf{x} \in \Omega \quad (3)$$

$$\theta(\mathbf{x}, t) = \theta_s(\mathbf{x}) \quad \mathbf{x} \in \Gamma_\theta, \quad q(\mathbf{x}, t) \equiv \frac{\partial \theta(\mathbf{x})}{\partial n} = q_s(\mathbf{x}) \quad \mathbf{x} \in \Gamma_q \quad (4)$$

where θ_s and q_s represent the steady boundary temperature and the steady boundary heat flux, and \mathbf{n} denotes the

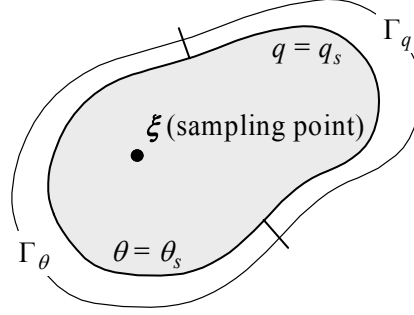


Figure 1. Schematic diagram of inverse measurement of thermal boundary conditions.

outward unit vector normal to the boundary.

Under these assumptions, the problem is to identify the temperature θ_s on Γ_θ and heat flux q_s on Γ_q from a transient temperature history measured at ξ within the domain, as shown in Figure 1.

3. IDENTIFICATION METHODOLOGY

For convenience in representing the integral equations derived later, we denote eqn.(2) by using the linear operator \mathcal{L} , such that

$$\mathcal{L}[\theta(\mathbf{x}, t)] = 0, \quad \mathcal{L} \equiv \frac{\partial}{\partial t} - \nabla^2 \quad (5)$$

Let us now consider the weak form of eqn.(5), which can be expressed as

$$\int_{\Omega} \int_0^{\tau} \theta^* \mathcal{L}[\theta] dt d\Omega = 0 \quad (6)$$

where θ^* is a test function or an adjoint temperature and τ is the specific time. Applying integration by parts to eqn.(6), we obtain the following integral equation:

$$\int_{\Omega} \int_0^{\tau} \theta \mathcal{L}^*[\theta^*] dt d\Omega = \int_{\Gamma} \int_0^{\tau} (\theta^* q - q^* \theta) dt d\Gamma - \int_{\Omega} [\theta^* \theta]_0^{\tau} d\Omega \quad (7)$$

where q^* is the adjoint heat flux, and \mathcal{L}^* denotes the adjoint operator, which can be expressed as

$$\mathcal{L}^* = -\frac{\partial}{\partial t} - \nabla^2 \quad (8)$$

In order to eliminate the last term in the right-hand side of eqn.(7), we set the adjoint temperature at τ to zero, such as

$$\theta^*(\mathbf{x}, \tau) = 0 \quad \mathbf{x} \in \Omega \quad (9)$$

which can be regarded as an initial condition for the adjoint problem.

Here, we choose the following adjoint problem in order to evaluate the effects of thermal boundary conditions on the temperature measured at ξ and at τ .

$$\mathcal{L}^*[\theta^*(\mathbf{x}, t)] = \delta(\xi - \mathbf{x}) \delta(\tau - t) \quad (10)$$

$$\theta^*(\mathbf{x}, t) = 0 \quad \mathbf{x} \in \Gamma_\theta, \quad q^*(\mathbf{x}, t) = 0 \quad \mathbf{x} \in \Gamma_q \quad (11)$$

where $\delta(\cdot)$ is Dirac's delta function. Substituting eqns (9)-(11) into eqn.(7) under the steady boundary conditions in eqn.(4), we obtain the following boundary integral relationship:

$$\theta(\xi, \tau) = \int_{\Gamma_q} \left(\int_0^{\tau} \theta^*(\mathbf{x}, \tau - t) dt \right) q_s(\mathbf{x}) d\Gamma - \int_{\Gamma_\theta} \left(\int_0^{\tau} q^*(\mathbf{x}, \tau - t) dt \right) \theta_s(\mathbf{x}) d\Gamma \quad (12)$$

Equation (12) indicates that if we numerically solve the adjoint eqn.(10) under the initial and boundary

conditions in eqns (9) and (11), we can predict the temperature at ξ and at τ under arbitrary thermal boundary conditions.

Let us now consider an inverse problem, in which the thermal boundary conditions should be evaluated by a temperature history measured at ξ . In this study, we assume that the boundary is divided into N sub-boundaries, on each of which the thermal boundary condition is uniform. We also assume that we can obtain M ($M \geq N$) temperatures at ξ from the measured temperature history.

According to eqn.(12) under the assumptions above, we arrive at a discrete problem represented by a system of linear equations, such that

$$\mathbf{A}\mathbf{x} = \mathbf{b}, \quad \mathbf{A} \in \mathbb{R}^{M \times N} \quad (13)$$

where

$$\mathbf{A} = \begin{bmatrix} a_{11} & a_{12} & \cdots & a_{1N} \\ a_{21} & a_{22} & \cdots & a_{2N} \\ \vdots & \vdots & \ddots & \vdots \\ a_{M1} & a_{M2} & \cdots & a_{MN} \end{bmatrix}, \quad \mathbf{x} = \begin{bmatrix} x_1 \\ x_2 \\ \vdots \\ x_N \end{bmatrix}, \quad \mathbf{b} = \begin{bmatrix} \theta(\xi, \tau_1) \\ \theta(\xi, \tau_2) \\ \vdots \\ \theta(\xi, \tau_M) \end{bmatrix} \quad (14)$$

In the eqations above, x_n ($n = 1, 2, \dots, N$) are unknown temperatures on Γ_θ or unknown heat fluxes on Γ_q to be estimated. On the other hand, a_{mn} ($m = 1, 2, \dots, M$, $n = 1, 2, \dots, N$) are known coefficients that can be calculated as

$$a_{mn} = \begin{cases} -\int_{\Gamma_n} \int_0^{\tau_m} q^*(\mathbf{x}, \tau_m - t) dt d\Gamma & \Gamma_n \subset \Gamma_\theta \\ +\int_{\Gamma_n} \int_0^{\tau_m} \theta^*(\mathbf{x}, \tau_m - t) dt d\Gamma & \Gamma_n \subset \Gamma_q \end{cases} \quad (15)$$

by numerically solving the adjoint problem (10) under the homogeneous boundary conditions (11). Note that the solution of the adjoint problem in eqn.(10) converges rapidly in time, because it is an impulse response from a unit impulse at ξ . In other words, only the early stage of the solution is significant and the late stage is negligible. Thus, we can compute a_{mn} at arbitrary time τ_m using a truncated numerical solution.

Finally, from eqn.(13), the unknown thermal boundary conditions can be estimated by

$$\mathbf{x} = (\mathbf{A}^T \mathbf{A})^{-1} \mathbf{A}^T \mathbf{b} \quad (16)$$

in a least squares sense. It should be noted that the discrete system (13) derived from a Fredholm type integral equation (12) is very ill conditioned[3]; i.e., the condition number of the matrix \mathbf{A} is very large when the dimension of the system becomes large. Thus, we need a certain regularization method to stabilize the solution \mathbf{x} . About this issue, we will discuss later.

4. COMPUTATIONAL EXPERIMENTS

4.1 Identification Model and Numerical Method

In order to demonstrate the present method, we carried out computational experiments in a two-dimensional square body as shown in Figure 2, in which the bottom surface is heated with sinusoidal heat flux, while the side surfaces are insulated and the top surface is maintained at an initial temperature. In the computational experiments, the measured temperature history at ξ was numerically simulated by the finite difference method and is indicated in Figure 3.

To construct the coefficient matrix \mathbf{A} in eqn.(13), the adjoint problem (10) has to be solved under the homogeneous boundary conditions (11). According to eqn.(15), the elements of the coefficient matrix \mathbf{A} can also be computed from a step response using a steady heat source at ξ , the strength of which can be determined by assuming a finite heat source and by using the property of Dirac's delta function; i.e., the product of strength and area of the finite heat source should be unity. In this way, the adjoint problem was also computed by the finite difference method by setting a steady finite heat source at ξ .

4.2 Identification Results without Regularization

In the first trial, the bottom surface is divided into five sub-boundaries ($N_b = 5$), and we suppose that the boundary conditions on side and top surfaces are also unknown, although they are uniform. Thus, the total number of unknown variables is eight ($N = N_b + 3 = 8$).

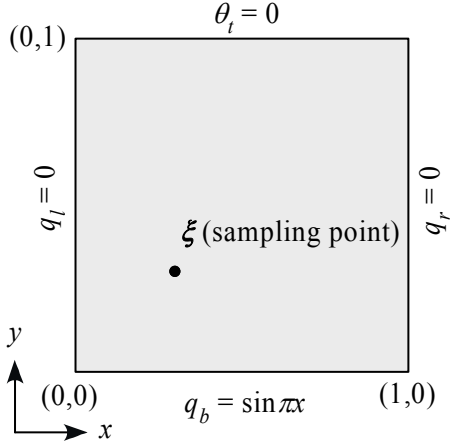


Figure 2. Identification model.

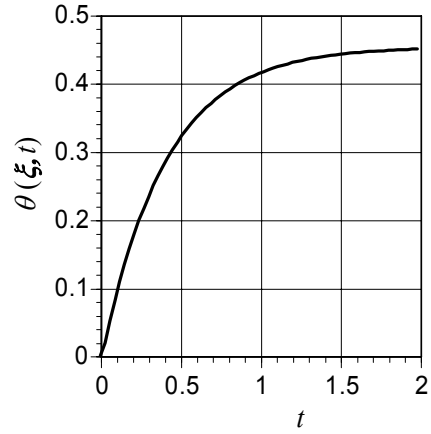
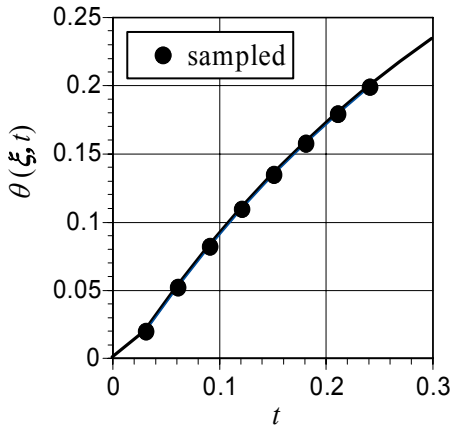
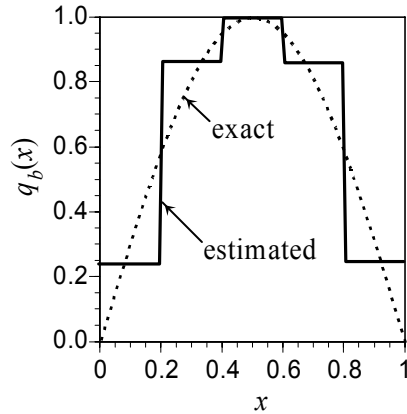


Figure 3. Temperature history obtained at ξ .



(a) sampled temperatures used for identification.



(b) estimated heat flux distribution on bottom surface (without regularization).

Figure 4. Identification result ($N_b = 5, N = 8$).

Table 1: Identification results on side and top surfaces
($N_b = 5, N = 8$, without regularization).

	q_l	q_r	θ_t
exact	0.0	0.0	0.0
estimated	1.58×10^{-4}	-9.31×10^{-4}	8.79×10^{-5}

Figure 4(a) shows the sampled temperatures for constructing the vector \mathbf{b} in eqn.(13). The estimated heat flux distribution on the bottom surface is shown in Figure 4(b), and the estimates on side and top surfaces are indicated in Table 1. The results on side and top surfaces are satisfactory, and the estimated heat flux distribution on the bottom surface is also good, although the resolution is very low.

Next, we tried to increase the number of sub-boundaries on the bottom surface to obtain higher resolution ($N_b = 10, N = 13$). Figure 5(a) shows the sampled temperatures for constructing the vector \mathbf{b} in eqn.(13), and the identification result on the bottom surface is shown in Figure 5(b). Unfortunately, the result is not acceptable, because the solution has many sign changes and the solution norm is much larger than the exact solution norm. These are typical phenomena appeared in the ill-posed problems. Therefore, we have to use a certain regularization method to stabilize the solution.

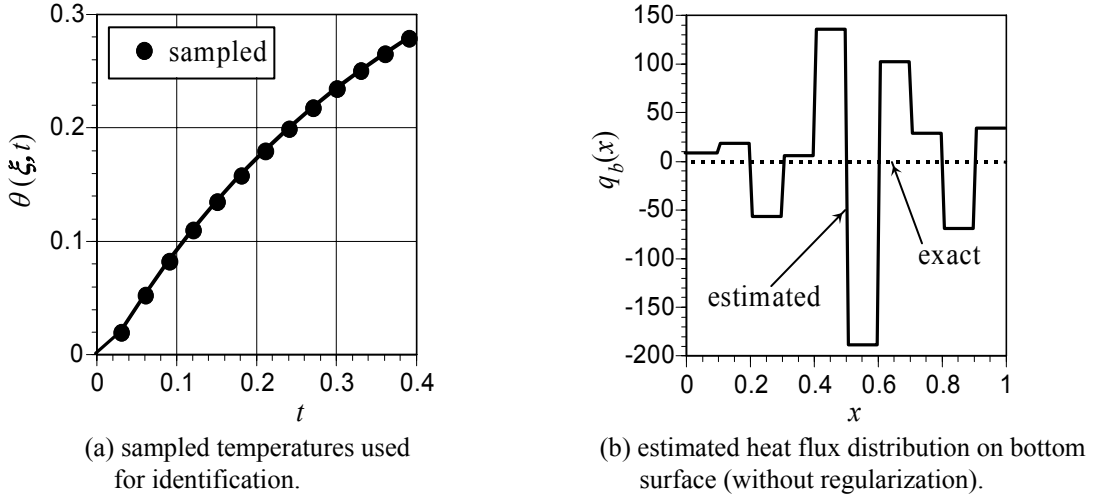


Figure 5. Identification result ($N_b = 10, N = 13$).

4.3 Identification Results with Tikhonov Regularization

In order to analyze the ill-posed characteristics appeared in the present approach, let us consider the least squares problem derived from the present identification process, such that

$$\min_x \|Ax - b\|_2, \quad A \in \mathbb{R}^{M \times N} \quad (M \geq N) \tag{17}$$

The SVD, singular value decomposition, is the useful tool to analyze the ill-posed problems[3]. The SVD of the coefficient matrix A is a decomposition of the form,

$$A = \sum_{n=1}^N u_n \sigma_n v_n^T \tag{18}$$

In this decomposition, the numbers σ_n are the singular values of A . Using the SVD, the least squares solution can be expressed as

$$x_{LSQ} = \sum_{n=1}^N \frac{u_n^T b}{\sigma_n} v_n \tag{19}$$

Generally, in the ill-posed problems, the singular values decay gradually to zero, and an increase of the dimension of A will increase the number of small singular values. Thus, the small singular values in the least squares solution amplify the data errors and rounding errors in the sampled data.

Figure 6 shows the distribution of the singular values for the present problem, and Figure 7 indicates the corresponding solution norms. Obviously, our problem shows the ill-posed characteristics when the number of unknown boundary values increases.

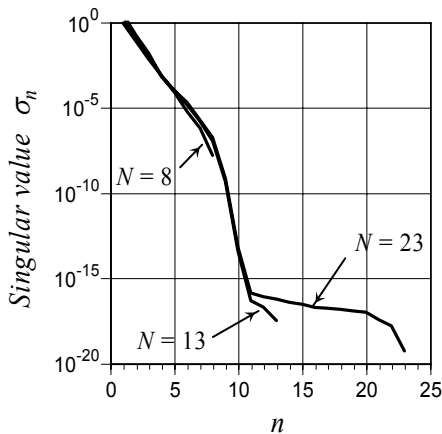


Figure 6. Distribution of singular values.

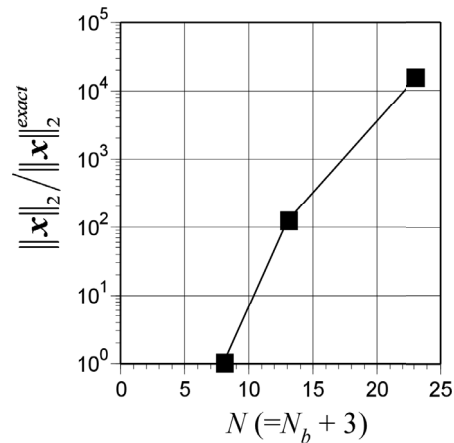


Figure 7. Solution norms (without regularization).

In this study, we adopted Tikhonov regularization method to stabilize the least squares solution. In Tikhonov regularization, the regularized solution is defined as,

$$\mathbf{x}_\lambda = \arg \min \left\{ \|\mathbf{Ax} - \mathbf{b}\|_2^2 + \lambda^2 \|\mathbf{x}\|_2^2 \right\} \quad (20)$$

where λ is the regularization parameter. Equation (20) minimizes the combination of the residual norm and the solution norm, and the regularization parameter controls the weight of them. Using the SVD, the regularized solution can be expressed as

$$\mathbf{x}_\lambda = \sum_{n=1}^N f_n \frac{\mathbf{u}_n^T \mathbf{b}}{\sigma_n} \mathbf{v}_n, \quad f_n = \frac{\sigma_n^2}{\sigma_n^2 + \lambda^2} \quad (21)$$

where f_n are called the filter factors, and the problem is how we choose the optimal regularization parameter λ .

The L-curve is a convenient graphical tool for choosing optimal regularization parameter. L-curve is a plot of a regularized solution norm versus the corresponding residual norm. Thus the L-curve shows the trade-off between the size of the solution and the quality of the fit. Figure 8 shows the L-curve for the present problem when the number of sub-boundaries is 13 ($N_b = 10, N = 13$). In the least squares sense, the residual norm should be decreased, but according to the L-curve, if the regularization is too small, the solution norm rapidly increases due to the ill-conditioned coefficient matrix. Thus, the optimal regularization parameter exists around the corner of the L-curve. To find the optimal regularization parameter corresponding to the corner of the L-curve, we calculated the curvature as a function of the regularization parameter, then we chose the optimal regularization parameter at the peak of the curvature, as shown in Figure 9.

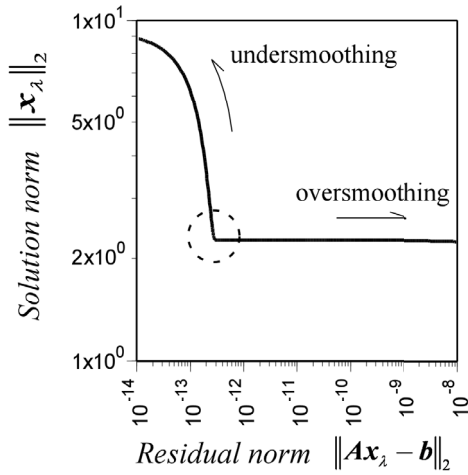


Figure 8. L-curve ($N_b = 10, N = 13$).

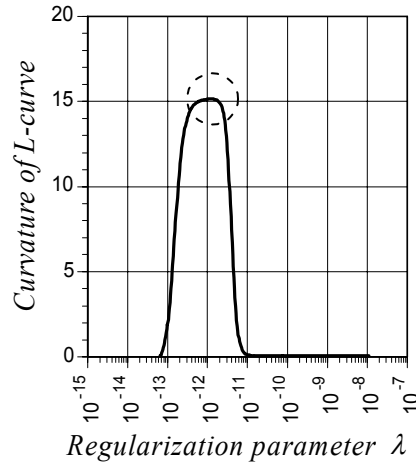


Figure 9. Curvature of L-curve ($N_b = 10, N = 13$).

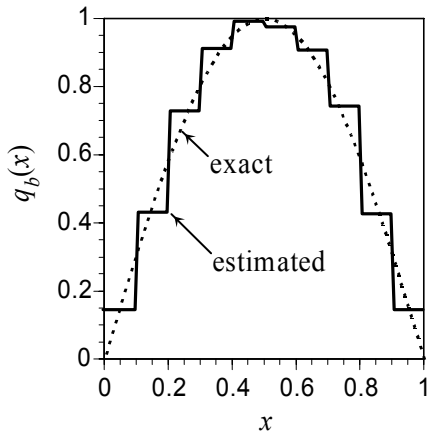


Figure 10. Estimated heat flux distribution on bottom surface ($N_b = 10, N = 13$).

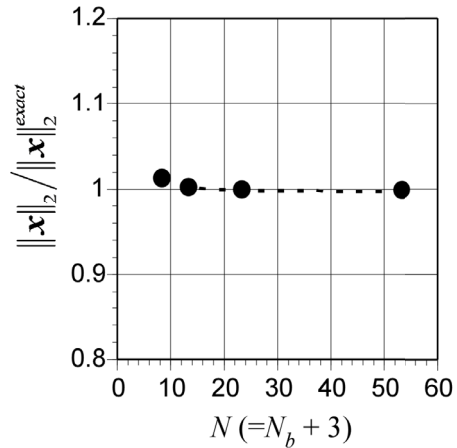


Figure 11. Solution norms (with regularization).

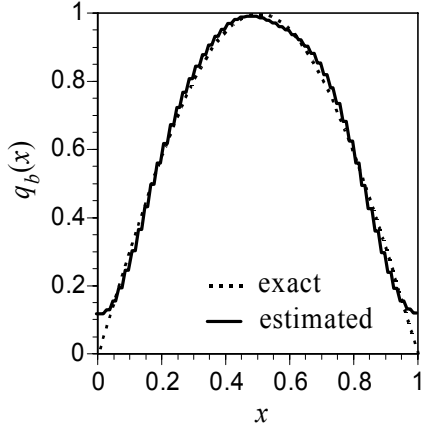


Figure 12. Estimated heat flux distribution on bottom surface ($N_b = 50, N = 53$).

Using the optimal regularization parameter, the previous result shown in Figure 5(b) can dramatically be improved as shown in Figure 10. Figure 11 demonstrates the effectiveness of the regularization. Using the regularization with the optimal regularization parameter, the solution norm, which is normalized by the exact solution norm, can be maintained at almost unity even when the number of sub-boundaries is greater than 50. Thus, we can estimate the heat flux distribution on bottom surface with enough resolution as shown in Figure 12 as well as the good estimates on side and top surfaces as listed in Table 2.

5. CONCLUSIONS

In this study, a non-iterative approach based on adjoint formulation of conduction heat transfer is proposed to identify the thermal boundary conditions from a transient temperature history measured in a solid body.

The main features of the present approach can be summarized as follows:

- (1) Introducing an adjoint problem and its associated Green's function, the relationship between the thermal boundary conditions and the measured temperature history can directly be obtained.
- (2) Using the numerical Green's function and assuming the step-wise profiles of the thermal boundary conditions, we can determine the thermal boundary conditions in the least squares sense.
- (3) Using Tikhonov regularization method and the L-curve criterion for choosing the regularization parameter, we can get good estimates of thermal boundary conditions even under ill-posed conditions.

Finally, it should be noted that we have so far neglected the measurement errors except for the rounding errors, and also neglected the time changes of the boundary conditions. From the practical point of view, however, these issues are very important. Now, we are trying to solve such a problem and searching more robust regularization method suitable for this kind of problem.

REFERENCES

1. O.M. Alifanov, *Inverse Heat Transfer Problems*, Springer-Verlag, New York, 1994.
2. J.V. Beck, B. Blackwell and C.R. St.Clair, *Inverse Heat Conduction: Ill-Posed Problems*, Wiley Intescience, New York, 1985.
3. P.C. Hansen, *Rank-Deficient and Discrete Ill-Posed Problems*, SIAM, Philadelphia, 1998.
4. Edited by H.R.B. Orlande, *Proceedings of the 4th International Conference on Inverse Problems in Engineering: Theory and Practice*, Vol.II, Brazil, 2002.

Table 2: Identification results on side and top surfaces (with regularization).

	q_l	q_r	θ_t
exact	0.0	0.0	0.0
$N = 13$	1.63×10^{-4}	1.56×10^{-4}	-2.26×10^{-5}
$N = 23$	1.63×10^{-4}	1.59×10^{-4}	-2.31×10^{-5}
$N = 53$	1.63×10^{-4}	1.60×10^{-4}	-2.32×10^{-5}